Evaluation of Interior Noise Control Treatments for Advanced Turboprop Aircraft

R. A. Prydz,* J. D. Revell,† F. J. Balena,‡ and J. L. Hayward§
Lockheed-California Company, Burbank, California

Experimental noise-reduction data have been obtained on a 43% scale model of a typical narrow-body aircraft. The acoustic performance of six sidewall "add-on" noise-reduction treatment designs has been evaluated under random and harmonic acoustic excitations and compared with predictions. A previously derived mathematical model for sound transmission into a stiffened cylindrical shell with multilayered treatments is used for the predictions. The theory compares favorably with experimental data at high frequencies and high-surface-density sidewall conditions, but underestimates low-frequency noise reduction. It is shown that add-on noise control treatment designs are effective in reducing the interior noise of propfan-powered aircraft to acceptable levels.

Introduction

RECENT analytical studies[1-8] have shown that acoustic treatment penalties of about 2% of aircraft gross weight are required to achieve acceptable interior noise levels (80 dBA) in high-speed propeller-driven aircraft. It was concluded that the double-wall mass law concept provided the most efficient noise-reduction technique for a given mass penalty. In these studies sidewall noise-reduction treatments are specified which are significantly heavier than current insulations used in aircraft cabin noise control. Clearly, it was desirable to obtain an experimental database for fuselage noise reductions which contained the appropriate range of frequency and sidewall treatment mass for theory validation. Such a test program was conducted by the Lockheed-California Company under sponsorship of the NASA Langley Research Center.[9] This paper presents the main results from Ref. 9. The test program, experimental data, and comparisons with theory contained herein represent a first step toward verification of the noise-reduction technology necessary to achieve acceptable cabin noise levels for propfan-powered aircraft. The test program was restricted to add-on designs which do not permit outer wall stiffening.

Experimental Investigation

Test Article

The fuselage structure used for this study was taken from a Fairchild Swearingen Metro 2—a 19-passenger commuter aircraft. The cylindrical fuselage section is 1.68 m in diameter and 9 m long. Table 1 gives the basic dimensions and section properties for the portion of the fuselage aft of the wing and forward of the cargo door, a distance of nearly 3.6 m. Since the rings and stringers are uniform and evenly spaced in this area, it was selected for the test section.

A support structure, end plates, an interior trim, and a floor structure were fabricated and installed in the fuselage section. The window and cargo door openings aft of the wing were also covered with 0.102-cm aluminum skin to simulate the mathematical model of Ref. 3 more closely. The interior fuselage structure, both floor and trim, were designed to provide the following conditions:

1) A very close simulation of a "floating" system, i.e., perfectly isolated, representative of the analytical model.

2) Physical connections to the fuselage wall, a configuration more representative of an actual aircraft.

In the floating configurations, the floor and inner wall structures were supported by eight airmounts mounted below the floor as shown in a sketch in Fig. 1. In the attached configurations the 1.9-cm-thick plywood floor was rigidly connected to the fuselage frames along the full length of the structure. Aluminum brackets, which were riveted to the frames just below the floor, were used to provide the rigid floor attachment. The inner wall consisted of partial cylindrical sections simulating trim panels, 0.089-cm thick and 1.22-m wide. To support the weight of the add-on material without causing buckling, the stiffness of each panel was increased by riveting structural angles to the ends. The trim panels were soft mounted to the floor. There were no other connections made except in the case where vibration isolators were also introduced between the frames and trim panels.

Test Configuration

The sound transmission tests were performed on the fuselage test model with various combinations of add-on material on the outer and inner walls including a baseline (bare) double-wall configuration. A sketch of the double-wall structure is shown in Fig. 1.

A total of nine double-wall configurations were evaluated for their sound transmission properties. These are listed in Table 2. The first six are the basic test configurations with the floating floor and trim. From these the effects of add-on mass were determined and compared with predictions.

Configurations 7-9 are identical to configuration 5 except for the floor and trim attachment conditions. These were used to evaluate the effects of a rigidly attached floor and a trim panel vibration isolation system designed for optimum performance. Vibration isolators were introduced between the inner and outer walls but only in the area of the test section. A total of 60 isolators were installed above the floor, 6 on each of the 10 frames along the test section.

Facility and Test Setup

The sound transmission tests were conducted in the acoustic facility of the Lockheed Kelly Johnson Research and Develop-

Presented as Paper 83-0693 at the AIAA 8th Aeroacoustics Conference, April 12-14, 1983; received Oct. 24, 1984; revision received Feb. 11, 1985.

*Research and Development Engineer.
†Research and Development Scientist. Associate Fellow AIAA.
‡Research and Development Scientist. Member AIAA.
§Scientist Research Senior.

ment Center. The test chamber has inside dimensions $5.8 \times 5.8 \times 4.3$ m and is completely lined with fiberglass wedges 1.5-m deep, providing free-field conditions down to 60 Hz. A 60-ft-long track allowed the fuselage model to be positioned for acoustic excitation in the center of the chamber or for reconfiguration outside. A schematic diagram of the test setup is shown in Fig. 2. It is seen that the 9-m-long test article fitted well within the confines of the facility but not without extending beyond the inner boundaries of the anechoic chamber. However, this did not compromise the setup for the sound transmission tests in any way. Flanking transmission measurements showed that the exterior sound levels at the two ends were nearly 40 dB lower than the peak excitation level measured at the center of the test section.[9]

The noise source was positioned 1.3 m from the surface of the fuselage midway between the boundaries of the test section, thus encompassing an incidence angle range of ± 0.97 rad (± 55.7 deg). The lateral dimension of the noise source corresponded to a propeller tip clearance of 0.8 diam, a value assumed for the narrow-body propfan of Ref. 2.

Test Procedures

Method of Excitation

A block diagram of the acoustic excitation system is shown in Fig. 3. The system consisted of a 2-kW electropneumatic generator (air modulator) coupled to a 20×40 deg cellular exponential horn with a 300-Hz cutoff frequency, a 300-W power amplifier, a one-third-octave-band equalizer, and two different signal generators. This particular sound system was selected because of its directivity, frequency, and amplitude characteristics, providing a close simulation of the propfan noise signature according to Ref. 2. A Gaussian random noise generator provided the signal for the broadband excitation. Before being amplified and reproduced, the signals were passed to the equalizer where they were adjusted. This was done to minimize the distortions in the harmonic propfan spectrum caused by the air modulator and to optimize the shape of the broadband spectrum for a maximum signal-to-noise ratio.

The two types of excitation spectra used for the sound transmission tests are shown in Figs. 4 and 5. These represent the peak free-field noise spectra measured without the presence of the fuselage test model on the axis of noise source, a distance of 1.3 m from the throat of the horn. As shown in Fig. 4, the harmonic spectrum is a close simulation of the estimated propfan spectrum whose full-scale levels and scaled frequencies are given in parentheses. The broadband spectrum, shown in Fig. 5, is reasonably flat over the frequency range of interest. It is noted that the slight fluctuations in the spectrum levels were caused by the one-third-octave filters of the equalizer. Figure 6 compares the noise source distribution with the estimated propfan noise signature. There is a reasonable collapse of the measured data for the two types of excitation and the agreement with prediction is fairly close.

Table 1 Outer wall structural properties of test article

Item	Values
Cylindrical structure	
Radius, m	1.68
Length, m	9.02
Skin thickness, cm	0.102
Surface density of skin, kg/m^2	2.78
Surface density skin plus stiffeners, kg/m^2	4.59
Frames	
Spacing, cm	38.1
Depth, cm	5.08
Cross-sectional area, cm^2	0.884
Area centroid (re: skin ℄), cm	2.835
Second area moment (re: skin ℄), cm^4	9.303
Torsion constant, cm^4	0.0030
Stringers	
Spacing, cm	18.3
Depth, cm	2.223
Cross-sectional area, cm^2	0.716
Area centroid (re: skin ℄), cm	0.772
Second area moment (re: skin ℄), cm^4	0.11904
Torsion constant, cm^4	0.00450

Table 2 Test configurations

Config. No.	Surface density, kg/m^2 Outer wall G_1	Inner wall G_2	Floor config.	Trim config.
1	4.59	2.25	Floating	Floating
2	4.59	7.13	Floating	Floating
3	4.59	12.01	Floating	Floating
4	9.47	2.25	Floating	Floating
5	9.47	7.13	Floating	Floating
6	9.47	12.01	Floating	Floating
7	9.47	7.13	Attached	Disconnected
8	9.47	7.13	Disconnected	Attached
9	9.47	7.13	Attached	Attached

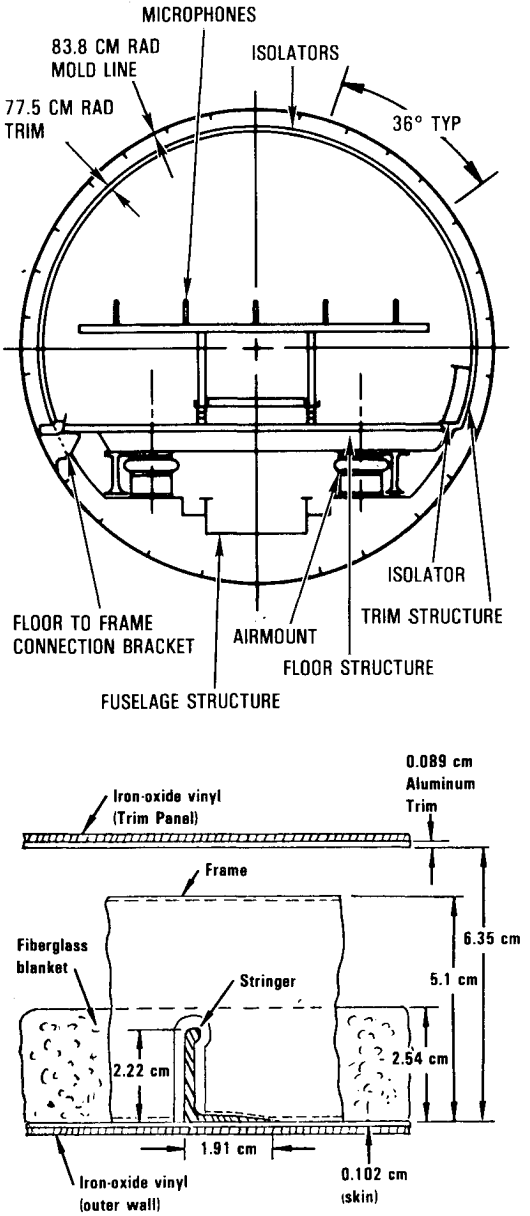

Fig. 1 Fuselage and sidewall cross sections.

Sound Transmission Measurements

The layout of the measurement locations is shown in Fig. 7. A total of 75 interior measurements were made for each test condition; i.e., two complete surveys for each of the nine test configurations, one for the simulated propfan excitation, and the other for broadband noise input. The interior sound field was measured with an array of five 1.3-cm B&K type 4165 condenser microphones mounted across the cabin on a movable support. The interior microphones were located 43 cm above the floor at a scaled height representing ear level for a seated passenger. The five radial measurements were repeated at 15 equally spaced axial stations, 0.46 m apart, over a distance of 6.44 m extending well beyond the boundaries of the test section. Axial positioning of the array was done manually from the outside of the facility as illustrated in Fig. 2. During testing two additional microphones were used for monitoring the external sound field. A high-intensity microphone, Endevco Model 8550M1, was installed in the throat of the horn of the noise generator and a 1.3-cm B&K microphone was positioned on the axis of the noise source, 15 cm from the fuselage.

Fuselage interior noise data and the data from the free-field measurements were used to determine noise reduction. In this study the noise reduction (NR) was defined as the difference between the peak free-field sound pressure level and the interior sound pressure level. The free-field level was measured at a distance 1.3 m from the noise source, coinciding with the surface of the fuselage when present. It is noted that this differs from the usual definition of noise reduction given as the difference between the sound pressure levels on the two sides of a structure. Also, it is not strictly an insertion loss since the input and output levels are not measured at the same point in space. Convenience and compatibility with prediction procedures were the main reasons for using this particular method to measure the noise reduction.

Both local and spatially averaged narrowband noise reductions were obtained. Spatial averages were determined in the radial as well as longitudinal directions by averaging the data over five different positions. Longitudinally averaged noise-reduction data were obtained for the two microphones closest

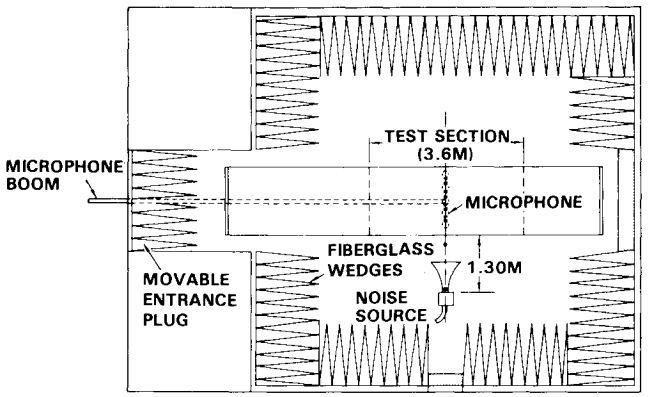

Fig. 2 Sound transmission test setup in anechoic chamber (plan view).

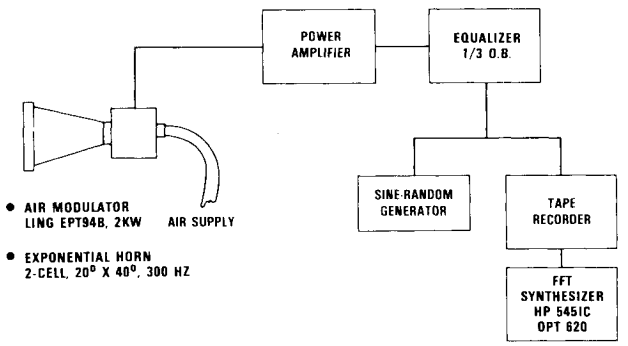

Fig. 3 Acoustic excitation system.

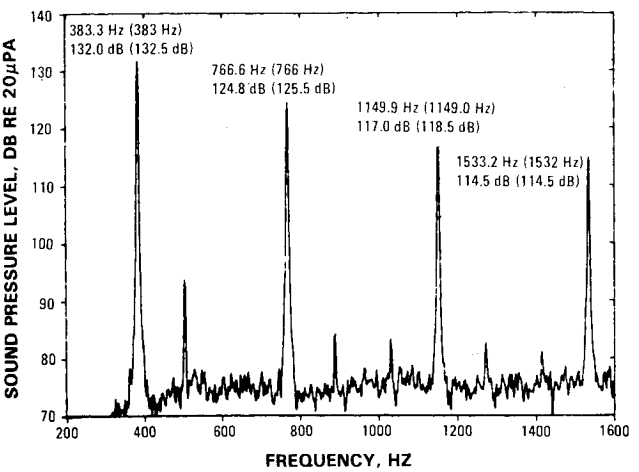

Fig. 4 Simulated propfan acoustic excitation spectrum measured in the free field on the noise source axis, 1.3 m from the source.

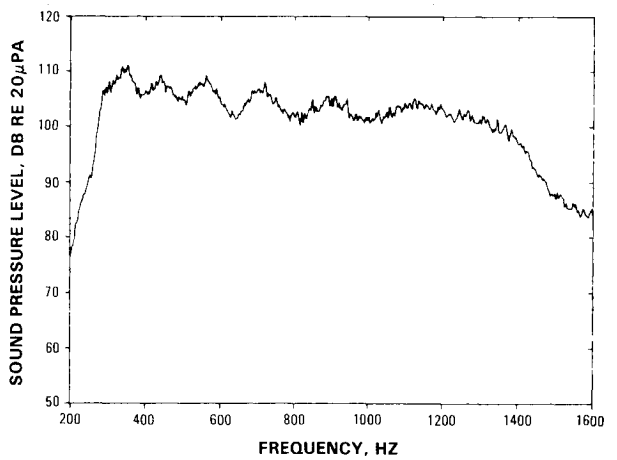

Fig. 5 Random acoustic excitation spectrum measured in the free field on the noise source axis, 1.3 m from the source.

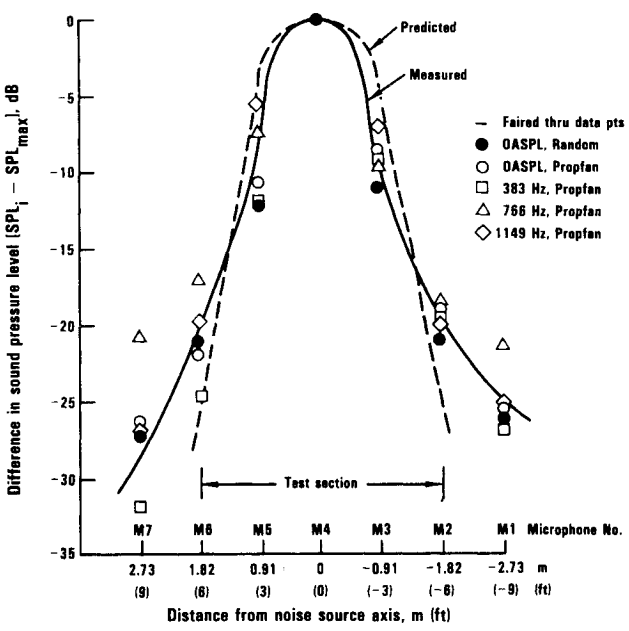

Fig. 6 Source noise distribution.

to the sidewall (M1 and M5) at axial stations 2, 1, −1, and −2 (see Fig. 7). Radially averaged data from all five microphones across the cabin were obtained at each of the above stations. All data were analyzed in narrowband frequencies using a 2.4-Hz bandwidth.

Main Test Results

Figure 8 compares the narrowband noise reductions in the 250-1400-Hz frequency range for configurations 1-3 with the baseline (bare) outer wall. It is seen that the two add-on configurations (2 and 3) performed considerably better than configuration 1 with the untreated interior trim, particularly above 700 Hz where the differences in noise reduction are more than 15 dB. The minimum noise reduction occurs in the 350-450-Hz frequency range for all three configurations. Above 600 Hz the noise reduction increases at a rate of slightly less than 12 dB per octave for the two add-on configurations. The trend for the bare configuration is somewhat different. There is a broad dip in the noise-reduction curve around 900 Hz, followed by an increase with frequency similar to the trends of the add-on configurations. From these results it is also seen that an increased of the trim panel surface density from 7.13 to 12.01 kg/m^2 (configurations 2 and 3, respectively) provides a modest noise-reduction improvement of about 4 dB over the given frequency range.

The results of the configurations with the increased outer wall surface weight density are shown in Fig. 9. Similar to the bare outer wall cases, the first layer of add-on material on the trim panels produced a large increase in the noise reduction at most frequencies. However, as expected, a second layer of add-on material did not result in a significant improvement, less than what had been achieved for the corresponding configuration (3) with the baseline outer wall. In the 250-1000-Hz frequency range the rate of increase in the noise reduction for add-on configurations 5 and 6 is nearly 18 dB per octave as compared to 12 dB per octave for add-on configurations 2 and 3 with the baseline outer wall. Above 1000 Hz, in a region where the noise reduction approaches 75-80 dB, the slope decreases as the signal-to-noise ratio becomes the limiting factor.

The apportionment of the add-on material between the inner and outer walls is an important factor. Figure 10 compares the noise reduction of the two configurations (3 and 5) with the same total sidewall surface density. It is seen that the configuration with all of the treatment on the trim panels is less effective than the configuration with the add-on mass equally divided between the inner and outer walls. This is particularly true at frequencies about 700 Hz. These measured results are consistent with analysis,[2] which has shown that the best performance is achieved in an add-on double-wall design when both the trim and outer wall mass are equal.

Thus far, only the results of ideal configurations consisting of a "floating" (perfectly isolated) floor/trim structural system have been presented. The effects of attaching the floor rigidly to the fuselage frames and introducing vibration isolators between the outer wall and trim panels have also been experimentally investigated. The main findings of these experiments are:

1) Rigid attachment of the floor to the fuselage frames produced a small decrease in the noise reductions below 800 Hz and a large decrease at the higher frequencies (Fig. 11).

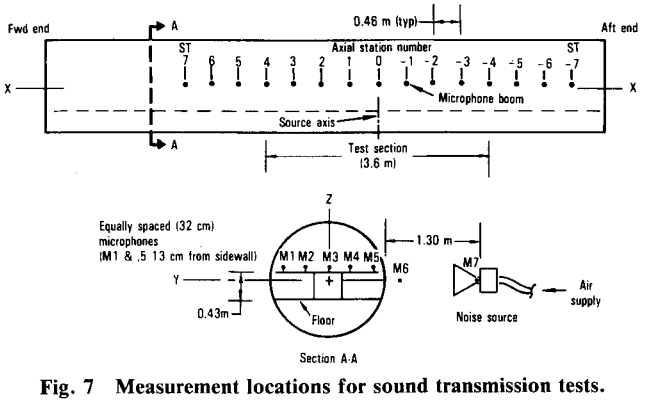

Fig. 7 Measurement locations for sound transmission tests.

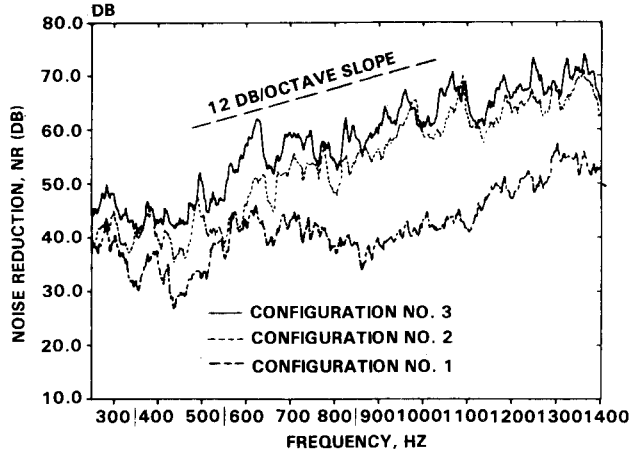

Fig. 8 Comparison of configurations with bare outer wall, longitudinally averaged noise reduction of microphone 5 at axial stations 2, 1, 0, −1, and −2.

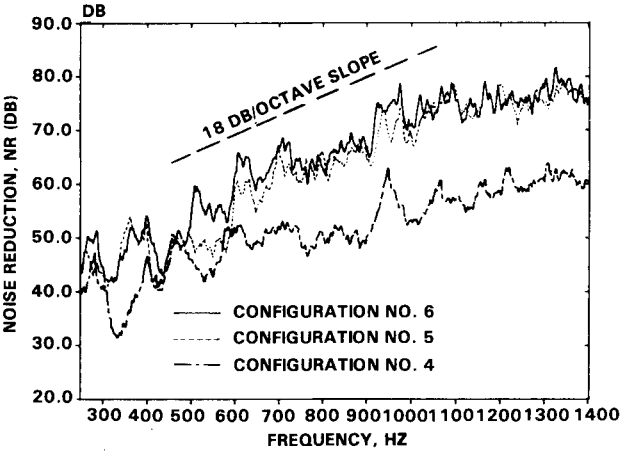

Fig. 9 Comparison of configurations with treated outer wall, longitudinally averaged noise reduction of microphone 5 at axial stations 2, 1, 0, −1, and −2.

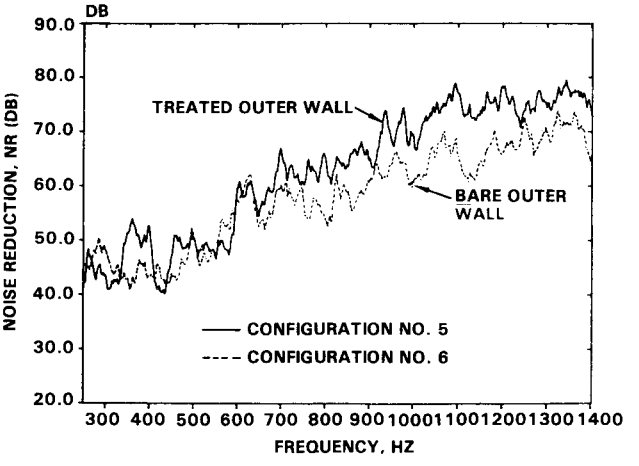

Fig. 10 Comparison of configurations with the same total surface density, longitudinally averaged noise reduction of microphone 5 at axial stations 2, 1, 0, −1, and 2.

2) Attachment of the trim panels to the fuselage frames by means of well-designed vibration isolators had no adverse effect on the interior noise levels (Fig. 12).

Comparison with Theory

Experimentally determined noise reductions for configurations 1-6 are shown with their respective theoretical values in Figs. 13-18. The prediction procedure used to obtain the theoretical values is described thoroughly in Refs. 2 and 9 and is based on earlier work by Koval[10,11] Beranek,[13] and Beranek and Work.[14] The envelope of interior noise data plotted to represent the experimental results was obtained from the five microphone radial array at positions 2, 1, 0, −1, and −2, as shown in Fig. 7. The reference external sound pressure level was assumed constant over the test section in the analyses and, therefore, would represent an average level 7 dB lower than the peak external level for the assumed propfan directivity shown in Fig. 6. The predicted noise reductions, which vary with angle of incidence, were an average of values over the length of the test section which represents an axial angle of incidence range of ±55.7 deg from the noise source axis. External inputs are limited to the 3.66-m length of the test section in the analysis, but the entire 9.0-m length of the test article is considered in the treatment of the interior. Absorptive material is assumed to be distributed evenly over the inner surface of the entire cylinder and the interior wave field is assumed to be finite at the center of the cross section. This is in contrast to the original Koval theory of Refs. 10 and 11 which assumes a singularity at the center which eliminates outwardly traveling waves. The interior absorption coefficient is assumed to be equal to 0.4 and constant with frequency.

An examination of Figs. 13-18 indicates that the predicted noise reduction tends to underestimate the measured noise reductions, especially at the low frequencies. The underestimation is greater when the outer wall is combined with a baseline trim panel (2.25 kg/m^2) as shown in Figs. 13 and 16. The comparisons improve at the low frequencies as the trim panel mass is increased and the best overall agreement is obtained with the heaviest trim panels as shown in Figs. 15 and 18. Since a narrow-body propfan would have a scaled blade passage frequency around 383 Hz, the theory would provide a fairly accurate but slightly conservative estimate of the sidewall noise reduction. Figures 13-15 show that most of the differences in Fig. 8 are explicable. The difference between the measured noise reduction of configurations 1 and 2 is greater than theory above 700 Hz by several decibels. Increased trim panel damping is a likely cause for the discrepancy. For add-on configurations 2 and 3, the difference in measured noise reduction agrees closely with the predicted results shown in Figs. 14 and 15. The broad dip in the noise-reduction curve for configuration 1, centered around 900 Hz, may be related to the ring frequency effect. It is well known[10-12] that for cylindrical structures with a single wall the noise reduction tends toward a minimum near the ring frequency, depending on the angle of incidence. However, this effect is much less pronounced, and often negligible, for double-wall cylinders when the inner wall is reasonably damped or noncylindrical, as evident from the present results or the results of Ref. 12.

Similarly there is a close correspondence between the predicted results shown in Figs. 16-18 and the differences in

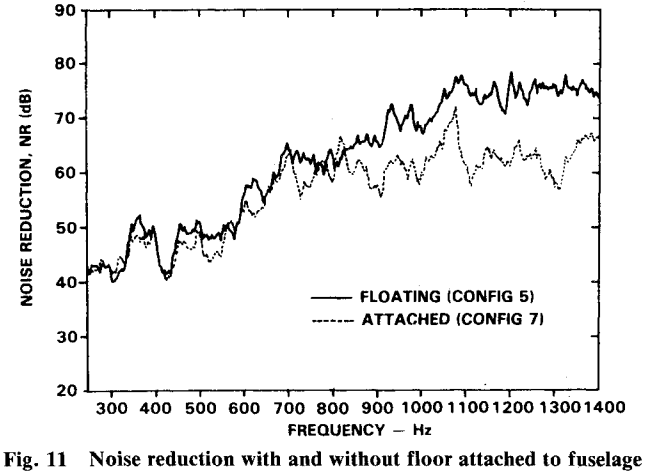

Fig. 11 Noise reduction with and without floor attached to fuselage frames.

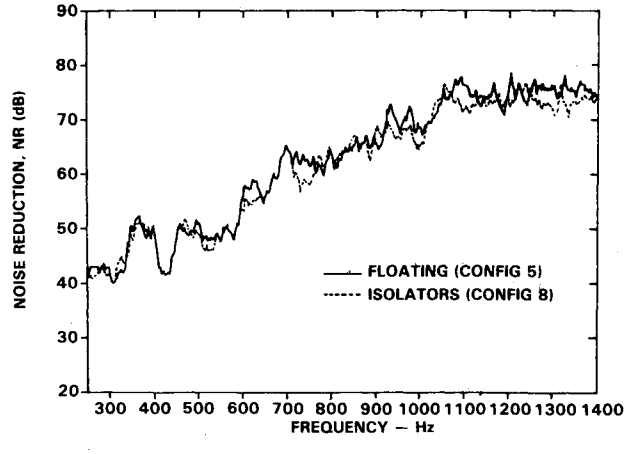

Fig. 12 Noise reduction with and without trim panel vibration isolators connected.

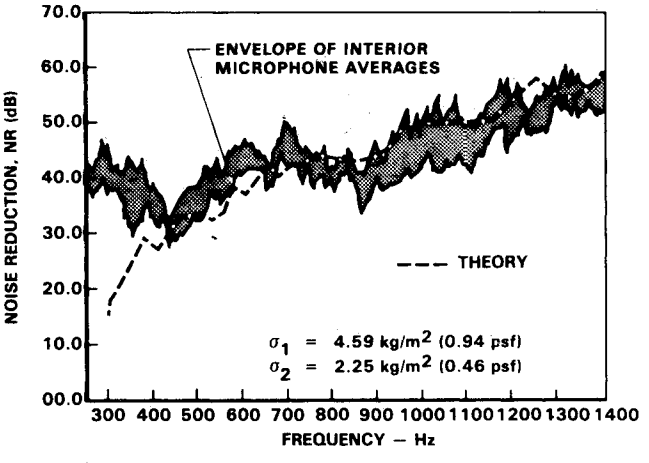

Fig. 13 Comparison between theory and experiment for configuration 1.

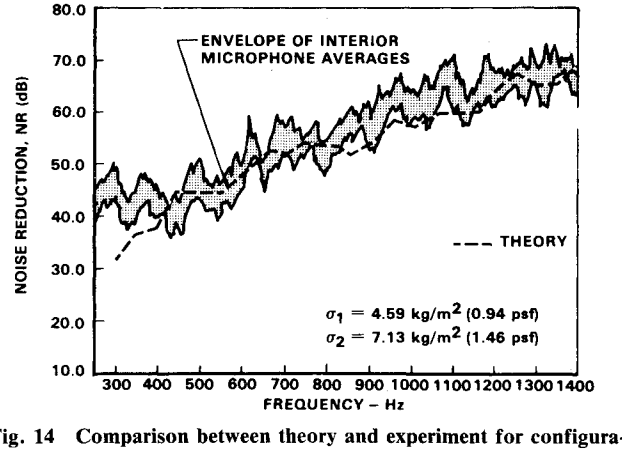

Fig. 14 Comparison between theory and experiment for configuration 2.

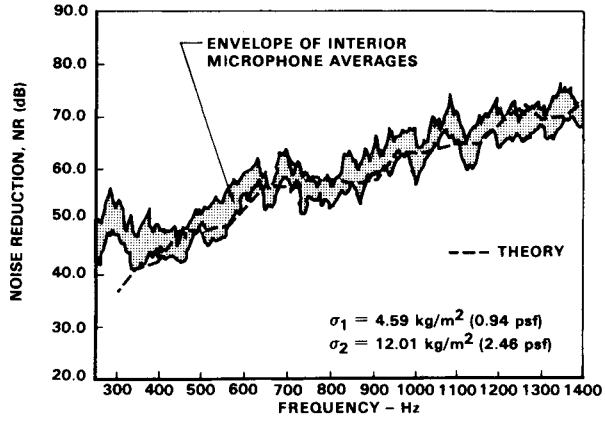

Fig. 15 Comparison between theory and experiment for configuration 3.

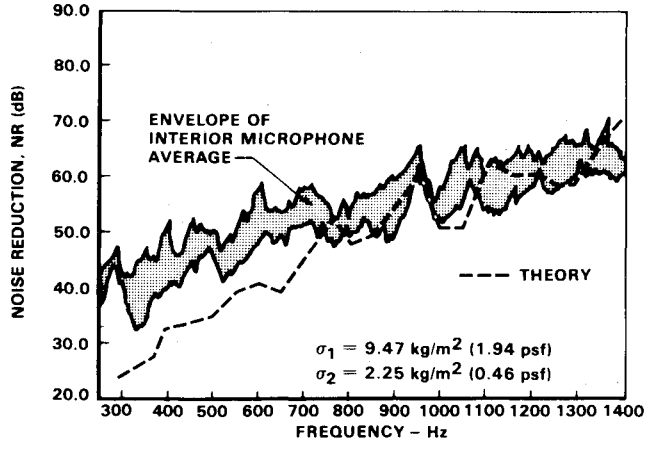

Fig. 16 Comparison between theory and experiment for configuration 4.

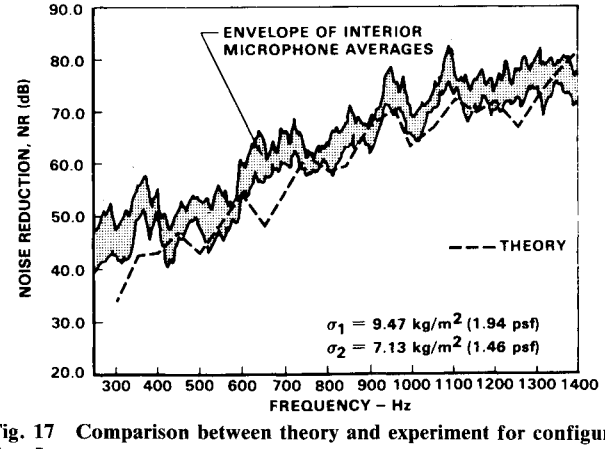

Fig. 17 Comparison between theory and experiment for configuration 5.

measured noise reduction for the treated outer wall cases shown in Fig. 9. The small changes in noise reduction between configurations 6 and 5 were expected since the trim panel surface density ratio is only 1.68 (Table 2). In contrast, the same ratio for configurations 5 and 4 is 3.2 which largely explains the greater differences shown in Fig. 9.

The current theory is being modified to incorporate features which offer the potential to improve low-frequency noise-reduction predictions. In general, the modifications being considered involve a more realistic treatment of the interaction between the vibrating structure and the interior sound field,

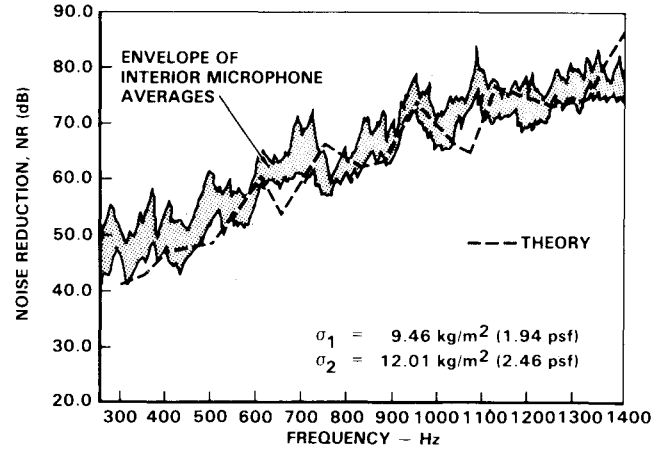

Fig. 18 Comparison between theory and experiment for configuration 6.

and a discrete stiffener analysis to replace the currently used smeared stiffener analysis of the cylinder.

Concluding Remarks

The present study provides a unique experimental database of noise-reduction measurements obtained for six double-wall sidewall treatment designs. These six configurations included three trim panel surface densities in conjunction with two different values of outer wall surface density and provided very high noise reduction compared to conventional aircraft fuselage sidewall construction. The test article, with a 1.68-m-diam fuselage, represents a 43% scale model of the narrow-body aircraft studied in Ref. 2; however, it differs to some extent in structural detail (in particular, in the spacing of stiffeners and the skin thickness). Despite the differences in structural detail between the exactly scaled narrow body of Ref. 2 and the present test article, calculations indicate similar trends of noise reduction vs added sidewall surface density, and roughly comparable absolute values of noise reduction vs total sidewall surface density.

The experimental data for the test article show fairly good agreement with the theory, although the theory tends to underestimate the measured noise reduction, especially at low frequencies. These results are encouraging in that they imply an increased likelihood of achieving the current noise-reduction objectives for propfan-powered aircraft with an acceptable mass penalty. Therefore, the tests have provided an important first step toward demonstrating the achievement of mass-efficient, high-noise-reduction, double-wall designs. Also, the data provide valuable information for evaluating double-wall transmission loss theories.

Two additional accomplishments were 1) the demonstration of a successful vibration isolation method for the trim panels, and 2) an evaluation of sidewall and floor attachment effects. A soft isolator design was specified, tested, and found to be successful in that no significant degradation of noise reduction occurred when the isolators were connected. The attachment of the floor showed some deterioration of noise reduction; however, this occurred mainly at frequencies exceeding twice the blade passage frequency of a typical propfan application. Therefore, this is considered to be a minor problem that would not impact the desired interior noise levels, and, if necessary, could be dealt with by exercising some care in vibration isolation design via routine engineering practice.

With respect to propfan-powered aircraft applications, the tests successfully simulated the harmonic spectrum of the exterior noise, according to a 1977 specification, using an air modulator/horn in an anechoic chamber. Furthermore, the noise reductions based on broadband excitation and narrow-band analysis were found to be very close to the noise-reduction values measured with sinusoidal excitation at the

first three multiples of blade passage frequency as shown in Ref. 9.

References

[1]Revell, J. D. and Tullis, R. J., "Fuel Conservation Merits of Advanced Turboprop Transport Aircraft," NASA CR 152096, Aug. 1977.

[2]Revell, J. D., Balena, F. J., and Koval, L. R., "Interior Noise Control by Fuselage Design Techniques on High-Speed Propeller-Driven Aircraft," NASA CR 159222, July 1980.

[3]Revell, J. D., Balena, F. J., and Koval, L. R., "Analysis of Interior Noise Control Treatments for High-Speed Propeller-Driven Aircraft," *Journal of Aircraft*, Vol. 19, Jan. 1982, pp. 31-38.

[4]Revell, J. D., Balena, F. J., and Koval, L. R., "Interior Noise Control by Fuselage Design for High-Speed Propeller-Driven Aircraft," *Journal of Aircraft*, Vol. 19, Jan. 1982, pp. 39-45.

[5]Revell, J. D., Balena, F. J., and Prydz, R. A., "Cabin Noise Weight Penalty Requirements for a High-Speed Propfan-Powered Aircraft: A Progress Report," SAE Paper 821360, Oct. 1982.

[6]Rennison, D. C., Wilby, J. F., Marsh, A. H., and Wilby, E. G., "Interior Noise Control Prediction Study for High-Speed, Propeller-Driven Aircraft," NASA CR 159200, Sept. 1979.

[7]Rennison, D. C., Wilby, J. F., and Wilby, E. G., "Prediction of the Interior Noise Levels of High-Speed Propeller-Driven Aircraft," AIAA Paper 80-0998, June 1980.

[8]Wilby, J. F., Rennison, D. C., Wilby, E. G., and Marsh, A. H., "Noise Control Predictions for High-Speed Propeller-Driven Aircraft," AIAA Paper 80-0999, June 1980.

[9]Prydz, R. A., Revell, J. D., Hayward, J. L., and Balena, F. J., "Evaluation of Fuselage Design Concepts for Interior Noise Control on High-Speed Propeller-Driven Aircraft," NASA CR 165960, Sept. 1982.

[10]Koval, R., "On Sound Transmission into a Thin Cylindrical Shell Under Flight Conditions," *Journal of Sound and Vibration*, Vol. 48, No. 2, 1976, pp. 265-275.

[11]Koval, L. R., "On Sound Transmission into a Thin Cylindrical Shell Under Flight Conditions," AIAA Paper 76-549, July 1976.

[12]Balena, F. J., Prydz, R. A., and Revell, J. D., "Single and Double Wall Cylinder Noise Reduction," *Journal of Aircraft*, Vol. 20, May 1983, pp. 434-439.

[13]Beranek, L. L., "Acoustical Properties of Homogeneous Isotropic Rigid Tiles and Flexible Blankets," *Journal of the Acoustical Society of America*, Vol. 19, July 1947, pp. 556-568.

[14]Beranek, L. L. and Work, G. A., "Sound Transmission Through Multiple Structures Containing Flexible Blankets," *Journal of the Acoustical Society of America*, Vol. 21, July 1949, pp. 419-428.